

Limits on the $K^+ \rightarrow \pi^+ + \nu + \bar{\nu}$ and $K^+ \rightarrow \pi^+ + n\gamma$ Decay Rates*

J. H. Klems† and R. H. Hildebrand

Enrico Fermi Institute and Department of Physics, The University of Chicago, Chicago, Illinois 60637

and

R. Stiening

Lawrence Radiation Laboratory, University of California, Berkeley, California 94707

(Received 8 February 1971)

The branching ratio for the process $K^+ \rightarrow \pi^+ + \nu + \bar{\nu}$ is shown by a counter-spark-chamber experiment to be less than 1.4×10^{-6} of all decay modes, assuming a pion energy spectrum like that of $K^+ \rightarrow \pi^0 + e^+ + \nu$. The apparatus was sensitive to pions in the kinetic-energy range 117–127 MeV. For the same energy interval a limit of 5×10^{-5} is established for the process $K^+ \rightarrow \pi^+ + \gamma + \gamma$, assuming a phase-space model for the decay. A limit of 4×10^{-6} is established for the process $K^+ \rightarrow \pi^+ + \gamma$.

I. INTRODUCTION

In earlier publications^{1,2} we have given preliminary results of an experiment to search for the decay processes $K^+ \rightarrow \pi^+ \nu \bar{\nu}$ and $K \rightarrow \pi^+ n\gamma$. We now present the final results and a detailed account of the work.

A. $K^+ \rightarrow \pi^+ + \nu + \bar{\nu}$

We have examined a sample of K^+ decays at rest for examples of

$$K^+ \rightarrow \pi^+ + \nu + \bar{\nu} \quad (1)$$

by looking for K -decay pions with an energy greater than those produced by $K^+ \rightarrow \pi^+ \pi^0$. We have observed no examples of the reaction. The apparatus was calibrated using pions from $K^+ \rightarrow \pi^+ \pi^0$. Since we observe only a part of the possible spectrum of π^+ energies in $K^+ \rightarrow \pi^+ \nu \bar{\nu}$, the upper limit on the branching ratio which is to be inferred from our measurement depends on the assumed shape of the pion spectrum (see Sec. III C). If we assume a first-order current-current interaction with constant form factors, then the three possible forms for the interaction and the corresponding limits (90% confidence) for the branching ratio $\Gamma(K^+ \rightarrow \pi^+ \nu \bar{\nu})/\Gamma(K^+ \rightarrow \text{all})$ are vector (1.4×10^{-6}), scalar (2.6×10^{-5}), and tensor (1.0×10^{-5}).

In an earlier experiment Camerini *et al.*³ established the limit 1.0×10^{-4} for the $K^+ \rightarrow \pi^+ \nu \bar{\nu}$ decay mode. Their apparatus was sensitive to π^+ in the energy ranges 0–105 and 114–127 MeV, which covered a sufficiently large fraction of the spectrum so that the result was insensitive to the form assumed for the interaction. An experiment to search for reaction (1) has also been proposed by Galaktionov and Shabalin.⁴

Reaction (1) belongs to a class of reactions which

should occur if neutral leptonic and hadronic currents simultaneously participate in weak interactions. These reactions would result if there were a term in the weak Hamiltonian of the form

$$(J_0 + S_0)\eta, \quad (2)$$

where $(J_0 + S_0)$ is a neutral hadronic current consisting of a $\Delta S = 0$ part (J_0) and a $|\Delta S| = 1$ part (S_0), and η is a neutral leptonic current. Experimentally it has been known for some time^{3,5–20} (see Table I) that if such a term exists it is suppressed relative to the known terms involving charged currents. The present upper limits^{12–18} on $K_{L,S}^0 \rightarrow \mu^+ \mu^-$ and $K_L^0 \rightarrow e^+ e^-$ are sufficiently low to exclude a term of the form (2) from any first-order theory, if one assumes that the matrix elements $\langle l^+ l^- | \eta | 0 \rangle$ and $\langle \bar{\nu}_i \nu_i | \eta | 0 \rangle$ ($l = \mu, e$) are of comparable magnitude (a type of lepton universality). Oakes²¹ has shown, however, that if $\langle l^+ l^- | \eta | 0 \rangle = 0$ but $\langle \bar{\nu}_i \nu_i | \eta | 0 \rangle \neq 0$, it is still possible to construct a theory in which the Hamiltonian contains a term of the form (2), and which is not contradicted by any of the experiments in Table I. His theory predicts²²

$$\Gamma(K^+ \rightarrow \pi^+ \nu \bar{\nu})/\Gamma(K^+ \rightarrow \text{all}) = 1.8 \times 10^{-5}$$

for a vector interaction. This is contradicted by the present experimental result.

Our result and the experiments in Table I thus indicate that a term of the form (2) should not be included in a first-order theory of weak interactions. Since it is known that in order to account for the empirical $|\Delta I| = \frac{1}{2}$ rule in strangeness-changing nonleptonic weak decays one must include neutral hadronic currents in the Hamiltonian,²³ one may take the viewpoint that the term (2) is absent because neutral leptonic currents are forbidden. This hypothesis might be tested by looking for neutral currents in purely leptonic interactions, such

TABLE I. Experimental limits on semileptonic decays involving neutral currents.

Reaction	Branching ratio ^a	Reference
$K^+ \rightarrow \pi^+ e^+ e^-$	$< 2.5 \times 10^{-6}$	5
	$< 4.4 \times 10^{-6}$	6
	$< 4 \times 10^{-7}$	7
$K^+ \rightarrow \pi^+ \mu^+ \mu^-$	$< 2.4 \times 10^{-6}$	6
	$< 3 \times 10^{-6}$	8
$K^+ \rightarrow \pi^+ \pi^0 e^+ e^-$	$< 8 \times 10^{-6}$	9
$K_L^0 \rightarrow \mu^\pm e^\mp$	$< 1 \times 10^{-4}$	10 ^b
	$< 9 \times 10^{-6}$	12
	$< 8 \times 10^{-6}$	11
	$< 1.9 \times 10^{-9}$	13
$K_L^0 \rightarrow e^+ e^-$	$< 1.6 \times 10^{-4}$	14
	$< 1.8 \times 10^{-5}$	12
	$< 1.5 \times 10^{-7}$	15
	$< 1.9 \times 10^{-9}$	13
$K_L^0 \rightarrow \mu^+ \mu^-$	$< 2 \times 10^{-4}$	14
	$< 1.6 \times 10^{-6}$	12
	$< 2.1 \times 10^{-7}$	15
	$< 2.6 \times 10^{-8}$	16
	$< 1.9 \times 10^{-9}$	13
$K_S^0 \rightarrow \mu^+ \mu^-$	$< 7.3 \times 10^{-6}$	17
	$< 7.3 \times 10^{-5}$	12
	$< 9.7 \times 10^{-5}$	18 ^c
$K^+ \rightarrow \pi^+ \nu \bar{\nu}$	$< 1.0 \times 10^{-4}$	3
	$< 1.4 \times 10^{-6}$	This work ^e
$\nu_\mu + p \rightarrow \nu_\mu + p$	$< 0.03\sigma(\nu_\mu + n \rightarrow \mu^- + p)$	19 ^d
$\bar{\nu}_e + d \rightarrow p + n + \bar{\nu}_e$	$< 60\sigma(\bar{\nu}_e + d \rightarrow n + n + e^+)$	20 ^b

^aRelative to all decay modes. Confidence level 90% except as noted.

^bThe authors do not state the confidence level. We infer it to be 63%.

^cConfidence level 63%.

^dThe authors do not state the confidence level. We infer it to be 90%.

^eSee Table III.

as $\nu_\mu + e^- \rightarrow \nu_\mu + e^-$. Alternatively, one might take the absence of (2) to mean that all neutral currents should be left out of the theory. In this case the nonleptonic $|\Delta I| = \frac{1}{2}$ rule must be considered a dynamical effect caused by the strong interactions²⁴ rather than a basic property of weak interactions. This viewpoint has the unattractive feature that each nonleptonic decay which obeys the $|\Delta I| = \frac{1}{2}$ rule must then have a separate explanation. At present one cannot decide between these two viewpoints.

Reaction (1) can also occur as a result of second or higher-order weak interactions. If the weak interaction has no characteristic mass (such as the mass of an intermediate boson), then on purely dimensional grounds one might estimate that the rates of second-order weak interactions are suppressed relative to kinematically similar first-order inter-

actions by a factor $\sim (GM_K^2)^2$. This results in an expected branching ratio of the order of 10^{-13} for reaction (1). A simple second-order application of weak-interaction theory as it is now known leads to a divergent result for the $K^+ \rightarrow \pi^+ \nu \bar{\nu}$ decay rate, and various theoretical studies²⁵ of higher-order weak processes have indicated that the rates for some of these processes may be enhanced above the values expected on dimensional grounds. The interpretation of our results for a second-order theory then hinges on the π^+ spectrum which the theory predicts for (1).²⁶

We note that if a "neutral current" reaction involving charged leptons, such as $K_L^0 \rightarrow \mu^+ \mu^-$, were observed to occur with a small branching ratio below the present empirical limits, it could be interpreted as resulting either from a second-order weak interaction or from a first-order weak interaction together with an electromagnetic interaction. For $K_L^0 \rightarrow \mu^+ \mu^-$, the dimensional argument given above leads to an estimate of $\sim 10^{-12}$ for the branching ratio by second-order weak processes, while a weak-electromagnetic model²⁷ for the decay predicts a branching ratio of order 10^{-8} . If $K_L^0 \rightarrow \mu^+ \mu^-$ were observed to occur with a branching ratio larger than 10^{-12} , one would be inclined to interpret it as a weak-electromagnetic interaction rather than a purely weak one, and the same is true of all other K decay modes which involve charged lepton-antilepton pairs. Thus the only K decay modes in which one might unambiguously observe a second-order weak decay are $K^+ \rightarrow \pi^+ \nu \bar{\nu}$, $K^- \rightarrow \pi^- \nu \bar{\nu}$, and $K^0 \rightarrow \pi^0 \nu \bar{\nu}$. Of these, $K^+ \rightarrow \pi^+ \nu \bar{\nu}$ appears to be the most accessible.

B. $K^+ \rightarrow \pi^+ + n\gamma$

In conjunction with our search for reaction (1), we have also searched for K^+ decays into π^+ and γ rays. We have observed no examples of this class of reactions.

The simplest such process which is allowed by angular-momentum conservation is $K^+ \rightarrow \pi^+ \gamma\gamma$. A previous search for this process has been reported by Chen *et al.*²⁸ Using an apparatus which was sensitive to pions of kinetic energy 60 to 90 MeV (kinematic limit = 127 MeV), they set an upper limit of 1.1×10^{-4} for the branching ratio into this decay mode. Our apparatus was sensitive to pions above approximately 117 MeV. Assuming a phase-space model for the decay, i.e.,

$$d\Gamma(K^+ \rightarrow \pi^+ \gamma\gamma)/dT_\pi = \lambda p_\pi,$$

where T_π and p_π are the kinetic energy and momentum of the pion and λ is a constant, we obtain a limit of 5×10^{-5} on the branching ratio.

The significance of this search has been dis-

cussed by Chen *et al.*²⁸ Briefly, they point out that a limit of $K^+ \rightarrow \pi^+ \gamma \gamma$ may be interpreted as a limit on the off-mass-shell behavior of the $K^+ \rightarrow \pi^+ \pi^0$ amplitude. It has been suggested that the $|\Delta I| = \frac{1}{2}$ law may be an exact selection rule for weak interactions, and that $K^+ \rightarrow \pi^+ \pi^0$ may occur because the $\pi^+ - \pi^0$ mass difference prevents the $\pi^+ \pi^0$ from being in a pure $T=2$ state. If we imagine that the two γ rays from the process $K^+ \rightarrow \pi^+ \gamma \gamma$ come from a virtual π^0 intermediate state, then for our energy range the $\pi^+ - (\gamma \gamma)$ mass difference is much greater than the $\pi^+ - \pi^0$ mass difference. According to this picture the rate for $K^+ \rightarrow \pi^+ \gamma \gamma$ may be greatly enhanced²⁹⁻³¹; however, the only specific model³² so far proposed for this mechanism predicts a rate in the region above $T_\pi = 117$ MeV, which is far below our experimental sensitivity. The vector-meson-dominant model^{33,34} and the η -pole model³⁵ also predict branching ratios much lower than the limit which we have been able to set in this experiment.

We can also set limits on the processes $K^+ \rightarrow \pi^+ n \gamma$ for $n > 2$, but since the phase-space spectrum is $d\Gamma/dT_\pi = \lambda p_\pi (T_M - T_\pi)^{n-2}$ [where $T_M =$ maximum energy of π^+], our experiment becomes less sensitive as n increases. For $n=3$,

$$\Gamma(K^+ \rightarrow \pi^+ + 3\gamma) / \Gamma(K^+ \rightarrow \text{all}) < 3 \times 10^{-4}$$

(90% confidence level).

Selleri has proposed a model³⁶ in which the K^+ has spin- $\frac{1}{2}$ and the strangeness-changing weak interactions violate angular-momentum conservation. His model would allow the process

$$K^+ \rightarrow \pi^+ + \gamma.$$

He predicts a branching ratio into this mode of 2×10^{-4} . Since in this case all of the π^+ would be produced above 117 MeV, we would be especially sensitive to this decay. We can place an upper limit (90% confidence level) on the branching ratio into this decay mode of

$$\frac{\Gamma(K^+ \rightarrow \pi^+ \gamma)}{\Gamma(K^+ \rightarrow \text{all})} < 4 \times 10^{-6}.$$

The previous upper limit³⁷ on this branching ratio was 1.5×10^{-4} .

II. THE EXPERIMENT

A. Principle of the Experiment

The experiment depends on the fact that no observed decay mode of the K^+ at rest produces π^+ with an energy above that of the π^+ from $K^+ \rightarrow \pi^+ \pi^0$ (109 MeV). Kinematically the K^+ may decay into a π^+ with energy up to 127 MeV, but to do so it must produce the π^+ in conjunction with a system with a rest mass smaller than that of the π^0 . The only possibilities for such a system are (i) γ rays,

(ii) e^+e^- pairs, (iii) $\nu\bar{\nu}$ pairs, and (iv) combinations of (i), (ii), and/or (iii). Since none of these systems involves strongly interacting particles, we expect the first-order reactions to predominate. These are $K^+ \rightarrow \pi^+ e^+ e^-$ (branching ratio $< 4 \times 10^{-7}$; see Table I), $K^+ \rightarrow \pi^+ \gamma \gamma$ (branching ratio $< 1.1 \times 10^{-4}$)²⁸ and reaction (1). (The process $K^+ \rightarrow \pi^+ \gamma$ is discussed in Sec. IB and Ref. 36.)

If we require a high-energy π^+ and also require that no γ rays or charged particles be produced going into the hemisphere opposite the π^+ , then we limit the possible reactions to $K^+ \rightarrow \pi^+ \nu\bar{\nu}$ and higher-order interactions (e.g., $K^+ \rightarrow \pi^+ \nu\bar{\nu} \gamma$). Conversely, the absence of such a high-energy π^+ is sufficient to exclude $K^+ \rightarrow \pi^+ \nu\bar{\nu}$.

It was necessary, therefore, to identify pions from K^+ decay with high reliability, to accurately measure their energy, and to detect with high efficiency associated charged particles and γ rays going into the opposite hemisphere. The apparatus which we designed to meet these requirements is shown in Fig. 1.

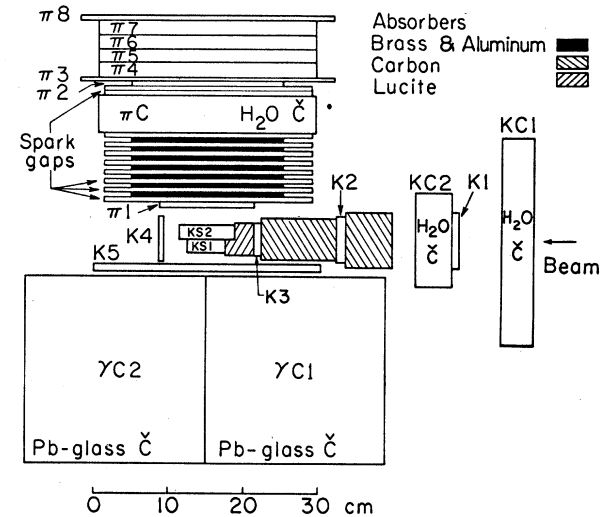


FIG. 1. Apparatus: Kaons stopping in the K -stop counters $KS1$ and $KS2$ are selected from the incoming beam by signals $\bar{K}C1$, $K1$, $\bar{K}C2$, $K2$, $K3$, $KS1$ and/or $KS2$, $\bar{K}4$, $\bar{K}5$ from the K telescope, where $K2$ and $K3$ have pulse heights $> 1.5 \times$ (pion pulse height). The threshold Čerenkov counters are triggered by beam pions but not by beam kaons. Decay particles which stop in the decay counters $\pi4-\pi7$ are selected by π telescope signals $\pi1$, πC , $\pi2$, $\pi3$, $\pi8$, $\bar{K}C1$, $\bar{K}C2$, $K4$, $K5$, where $\pi1$ is delayed > 6 nsec after $K3$. The πC counter is triggered by muons from $K^+ \rightarrow \mu^+ \nu$, but not by pions or muons which stop in the decay counters. Events which emit γ 's into the opposite hemisphere are eliminated by γ detector signals $\gamma C1$ and/or $\gamma C2$. Pions are distinguished from stopping muons by scope displays of the $\pi \rightarrow \mu \rightarrow e$ decay pulses in the decay counters. Removable absorber plates in the π detector allow selection of the decay-particle energy interval (see Fig. 4).

B. Description of the Apparatus

The K^+ were brought to rest in two small scintillation counters, and the decay pions (and muons) were observed by a π^+ detector placed perpendicular to the K^+ beam (see Fig. 1). A large lead-glass Čerenkov counter on the opposite side of the beam detected γ rays and fast charged particles. The π^+ detector consisted of a stack of spark chambers separated by brass and aluminum absorber plates of adjustable thickness, and followed by a stack of four scintillation counters ("decay" counters). The absorbers were normally adjusted so that π^+ of 115 to 145 MeV were brought to rest in the decay counters. Pions were identified by displaying the outputs of the four decay counters on two four-beam oscilloscopes and observing the $\pi^+ \rightarrow \mu^+ \rightarrow e^+$ decay sequence. One oscilloscope ("fast") had a 15-nsec/cm sweep speed and was used to detect the $\pi^+ \rightarrow \mu^+ \nu$ decay (~ 1.7 cm/ τ_π). The other ("slow") had a 0.37- μ sec/cm sweep speed and was used to detect the $\mu^+ \rightarrow e^+ \nu \bar{\nu}$ decay (~ 6 cm/ τ_μ).

The triggering logic, consisting of the K telescope, the π telescope, and the γ detector (see Fig. 1), selected events for which (i) a K^+ stopped in one of the " K -stop" counters, (ii) a charged particle later entered the π^+ detector and stopped in the decay counters, and (iii) no charged particles or γ rays were emitted in the opposite direction.

$$K^+ = K1, K2, K3, (KS1 \text{ and/or } KS2), \bar{K4}, \bar{K5}, \bar{KC1}, \bar{KC2},$$

where the bar indicates an anticoincidence. The $K1, K2, K3$ triple coincidence defined the incident K beam and discriminated in favor of K^+ on the basis of ionization [$(dE/dx)_K > 1.5(dE/dx)_\pi$]. The pulse heights in $KS1$ and $KS2$ indicated in which of these counters the K^+ stop occurred. Transmitted π^+ were suppressed by $\bar{K4}$. Pions which scattered in the K -stop counters were rejected by $\bar{K5}, \bar{KC1}, \bar{KC2}$, and by a timing requirement to be described below. The $\bar{K5}$ requirement also rejected K^+ which scattered and stopped in the face of the γ detector.

The π telescope selected from the K^+ decay products those charged particles which emerged from the absorber stack with low velocity and stopped in the decay counters. This was indicated by a "stop" signal:

$$\text{STOP} = \pi1, \pi2, \pi3, \bar{K4}, \bar{K5}, \bar{KC1}, \bar{KC2}, \bar{\pi C}, \bar{\pi 8}.$$

The $\bar{\pi C}$ requirement selected particles which emerged from the absorber plates travelling slowly, and served mainly to veto e^+ from $K^+ \rightarrow \pi^0 e^+ \nu$ and μ^+ from $K^+ \rightarrow \mu^+ \nu$. The $\bar{\pi 8}$ requirement then insured that the particle stopped in the decay coun-

Whenever the triggering logic selected an event, the oscilloscopes were triggered, the spark chambers were pulsed (after a 3.3- μ sec delay, to avoid interference with the oscilloscopes), and both spark chambers and oscilloscopes were photographed. The oscilloscope photographs were then scanned for events which exhibited the $\pi^+ \rightarrow \mu^+ \rightarrow e^+$ decay sequence. When such an event was found, it was possible to measure the range of the " π^+ " with good accuracy by following its path through the absorbers by means of the spark chambers and measuring the π^+ pulse height in the counter registering the $\pi^+ \rightarrow \mu^+ \rightarrow e^+$ decay.

The transmission of π^+ through the absorbers was measured by removing the γ detector from the triggering logic and measuring the $\Gamma(K^+ \rightarrow \pi^+ \pi^0) / \Gamma(K^+ \rightarrow \mu^+ \nu)$ branching ratio. The transmission determined in this way required only a small correction to be applicable to the search for reaction (1).

The beam, produced by the LRL Bevatron, consisted of π^+, K^+ , and p with an initial momentum of 500 MeV/ c . The amount of absorber necessary to stop the K^+ was sufficient to completely eliminate protons from the beam. It was therefore only necessary for the K telescope to identify K^+ and insure that they had stopped in one of the K -stop counters, and to suppress scattered and transmitted π^+ . This was accomplished with the following signal:

The $\bar{KC1}, \bar{KC2}$ requirement rejected beam π^+ which scattered into the π detector after a K^+ had stopped in one of the K -stop counters. Lead shielding placed around the beam upstream of the apparatus insured that all beam particles passed through $KC1$. The requirements $\bar{K4}, \bar{K5}$ suppressed decays with associated charged particles (e.g., $K^+ \rightarrow K^0$ by charge exchange in a K -stop counter, followed by $K_L^0 \rightarrow \pi^+ e^- \nu$; see Sec. III A 2). The absorber thickness used during the experiment was always much more than sufficient to stop π^+ from $K^+ \rightarrow \pi^+ \pi^0 \pi^0$ before they reached $\pi 2$.

Since the experiment depends upon searching for π^+ emitted with too high an energy to be consistent with $K^+ \rightarrow \pi^+ \pi^0$, it is essential that the K^+ decay at rest. In order to ensure this, the π telescope and the K telescope were operated in delayed coincidence in the following manner. The time of the K^+ signal was determined by the time the stopping K^+ passed through $K3$, and the time of the STOP signal was determined by the time the decay product passed through $\pi 1$. The K^+ signal was used to form a gate, K_D^+ , which was opened 6 nsec after the K^+

signal and had a duration of 48 nsec. The K_D^+ gate was then placed in coincidence with the π telescope. This requirement also suppressed scattered beam π^+ .

The triggering system as a whole was operated in either of two ways. The first way required that the decay product stop in the decay counters, but placed no restrictions on associated γ rays [i.e., it selected " $K^+ \rightarrow X^+ + (\text{neutral system})$ " events, where the X^+ stops in the decay counters]. This was used, for example, to measure $K^+ \rightarrow \pi^+ \pi^0$. We denote it by KX^+ :

$$KX^+ = (K_D^+, \text{STOP}).$$

The second way required in addition that no γ rays be detected by $\gamma C1$ or $\gamma C2$. This was the triggering mode used in searching for reaction (1). We denote it by $KX^+ \bar{\gamma}$:

$$KX^+ \bar{\gamma} = (K_D^+, \text{STOP}, \bar{\gamma C1}, \bar{\gamma C2}).$$

The counters $\gamma C1$ and $\gamma C2$ each consisted of a block of lead glass 12 in. (~15 radiation lengths) thick, viewed by a 60AVP photomultiplier tube. The inefficiency of these two counters was measured using the π^0 γ rays from $K^+ \rightarrow \pi^+ \pi^0$ and was found to be $(6 \pm 1) \times 10^{-4}$.

The outputs of the decay counters were displayed on both the fast and slow oscilloscopes. Since the

monoenergetic μ^+ produced in $\pi^+ \rightarrow \mu^+$ decay travels only about 1.6 mm in scintillator, few such decays will produce muons which leave the counter in which they originate. The electron produced in μ^+ decay, however, may have up to 52 MeV kinetic energy, and will usually leave the counter in which it originates. In order to improve $\pi^+ \rightarrow \mu^+$ identification for the special cases where the muon either decayed in $\pi 4$ producing an electron which went back through $\pi 3$, or decayed in $\pi 7$ producing an electron which went forward through $\pi 8$, pulses were displayed on the slow oscilloscope whenever a particle passed through $\pi 3$ or $\pi 8$ (see Fig. 3). A scintillation counter $K0$ was placed over the hole in the shielding through which the beam entered the experimental area. Any pulse in the slow oscilloscope which occurred in coincidence with a pulse from this counter (see Fig. 3) was assumed to be due to a scattered beam particle. The output of this counter was also used to monitor the instantaneous beam intensity and, by pulse height, to distinguish events for which two beam particles entered simultaneously.

C. Scanning and Measurement

1. Appearance and Identification of Events

Figures 2 and 3 show an example of a $\pi^+ \rightarrow \mu^+ \rightarrow e^+$

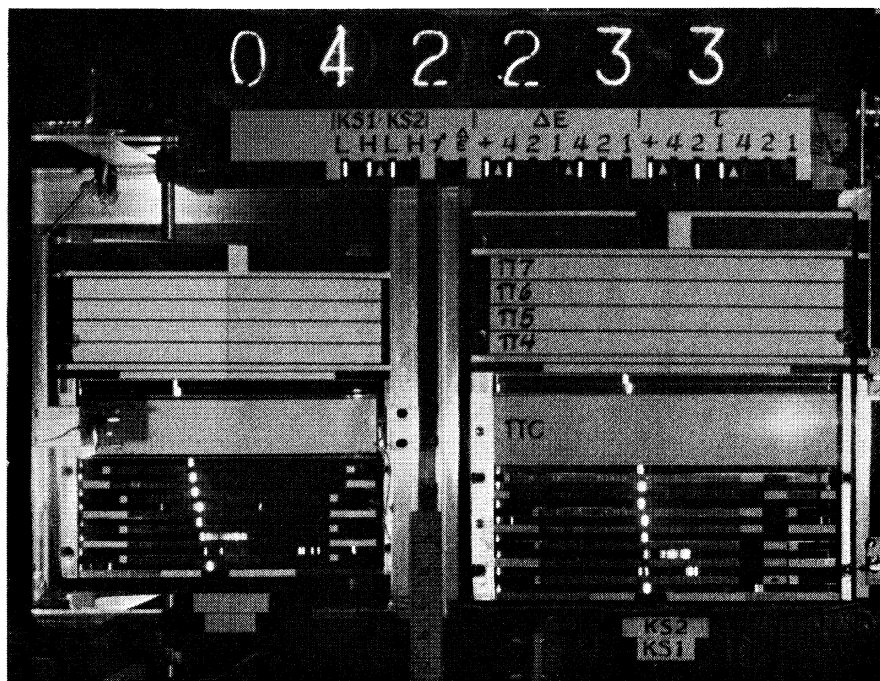


FIG. 2. A $\pi^+ \rightarrow \mu^+ \rightarrow e^+$ event from $K^+ \rightarrow \pi^+ \pi^0$ decay: Two views of the pion track traversing the spark gaps. The right-hand view looks directly at the downstream side of the apparatus; the left-hand view shows the bottom by means of a mirror. Note that the track appears to intersect the K -stop counters in both views. The row of labeled lights just below the event number contains coded information from the triggering system as explained in Sec. IIB.

decay, where the π^+ was produced by $K^+ \rightarrow \pi^+ \pi^0$. Figure 3 shows the characteristic signature of a pion. The signature begins with a sequence of pulses in the successive counters $\pi 3$, $\pi 4$, $\pi 5$, and $\pi 6$ (a "track") indicating the decay pion. This is followed by a single pulse of appropriate height, appearing in the fast scope in the counter $\pi 6$ where the pion "track" ends indicating a $\pi^+ \rightarrow \mu^+$ decay. Finally we see a "track" ($\pi 6$, $\pi 7$, and $\pi 8$) in the slow oscilloscope indicating the $\mu^+ \rightarrow e^+$ decay. Had the entering particle been a stopping μ^+ (e.g., from $K^+ \rightarrow \pi^0 \mu^+ \nu$), the appearance of the oscilloscopes would have been unchanged except that the fast oscilloscope would have shown only the entering track without the subsequent pulse in $\pi 6$.

After identifying the particle stopping in the decay counters, the scanner turns from the oscilloscope display to the spark-chamber display. For the event of Figs. 2 and 3 the digitized information in the spark-chamber display (see Fig. 2) indicates that the heavily ionizing K^+ stopped in $KS1$ and the

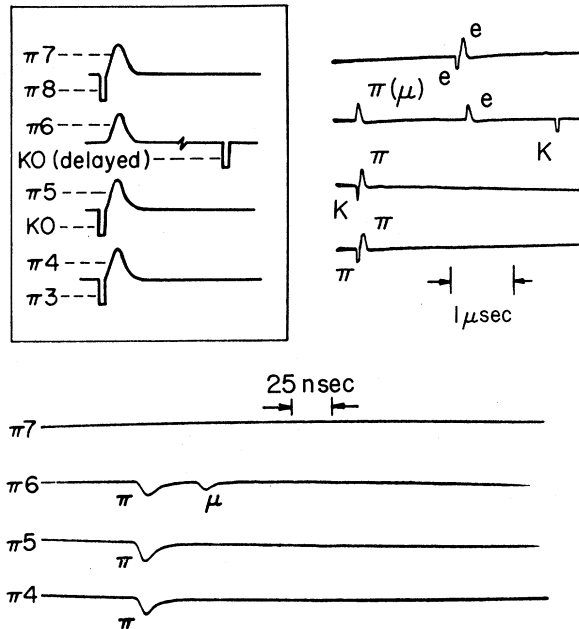


FIG. 3. A $\pi^+ \rightarrow \mu^+ \rightarrow e^+$ event from $K^+ \rightarrow \pi^+ \pi^0$ decay: Four-beam scope displays of the K , π , μ , and e pulses from counters $K0$ and $\pi 3$ – $\pi 8$. (Lower display – fast scope; upper right – slow scope.) The inset (upper left) shows how coincident pulses in all the counters would appear in the slow scope. (Pulses from $K0$, $\pi 3$, and $\pi 8$ are inverted and have fixed height.) The entry of the K^+ is marked by (prompt and delayed) pulses from $K0$. The pion "track," composed of pulses in $\pi 3$, $\pi 4$, $\pi 5$, and $\pi 6$ (pion stops in $\pi 6$), is seen at $t=0$. The $\pi^+ \rightarrow \mu^+$ decay is indicated (on fast scope) by a pulse at $t=37$ nsec in $\pi 6$, where the pulse height corresponds to the expected 4 MeV of the μ^+ . The $\mu^+ \rightarrow e^+$ decay is indicated (on slow scope) by an e^+ "track" at $t=1.6$ μ sec.

lightly ionizing π^+ produced by its decay passed through $KS2$, that there were no beam particles coincident with the K^+ , that associated γ rays were detected, and that the K^+ lifetime is reasonable (~ 12 nsec). We therefore conclude that it is an example of a K^+ decaying into a π^+ with associated high-energy γ rays. The additional knowledge that the triggering system was being operated in the KX^+ mode (see Sec. II B) when the picture was taken, and the subsequent measurement of the π^+ range, then indicates that the K^+ decay was $K^+ \rightarrow \pi^+ \pi^0$. Had the oscilloscope picture indicated that the stopping particle was a μ^+ rather than a π^+ , we would have concluded that the decay was (probably) $K^+ \rightarrow \pi^0 \mu^+ \nu$ or $K^+ \rightarrow \mu^+ \nu \gamma$.

2. Scanning Procedure and Criteria

The films showing the oscilloscope and spark-chamber pictures (see Fig. 2 and 3) were displayed on a pair of Recordak film viewers. Each frame of the oscilloscope film was scanned. When an event of interest was located, the spark-chamber film was then examined and the event recorded if it satisfied the scanning criteria.

An event was called a $\pi\mu e$ decay if it had the $\pi^+ \rightarrow \mu^+ \rightarrow e^+$ signature as described above, with the following qualifications: (i) an e which left a pulse in only a single counter was accepted only if it deposited more than 4.5 MeV in that counter, as measured by the pulse height; (ii) an e which occurred in coincidence with a $K0$ pulse was rejected; (iii) the e was required to occur before the spark chambers were fired (3.3 μ sec); (iv) the μ pulse was required to occur in the same counter in which the π stopped, and the e was required to originate in this counter; and (v) the μ pulse was accepted only if it was clearly resolved from the pulse made by the stopping π . All potential $\pi\mu$ decay pulses were measured and recorded regardless of pulse height. It was necessary, however, to set an arbitrary lower limit on pulse height in order to distinguish true pulses from tiny irregularities in the oscilloscope traces. This lower limit was taken to be slightly more than one-half the thickness of the trace. If an event satisfied the above criteria with the exception that there was no evidence of a $\pi\mu$ decay pulse in the fast scope, it was termed a μe decay.

Events termed $\pi\mu e$ or μe decays were recorded only if the corresponding spark chamber pictures satisfied three additional criteria: (i) the $KS1$ and $KS2$ lights had to indicate that a K^+ had stopped in the K stop counters; (ii) the track of the particle which stopped in the decay counters had to be clearly identifiable and measurable in the spark chambers; and (iii) the idealized track fit to the spark-

chamber track (as described below) had to intersect the K -stop counter in which the K^+ decay had occurred. About 10% of all " $\pi\mu e$ decays" were rejected by these additional criteria.

Condition (ii) rejected the same fraction ($\sim 4\%$) of decays for $\pi\mu e$ from $K^+ \rightarrow \pi^+ \pi^0$ and for μe from $K^+ \rightarrow \mu^+ \nu$. This ensured that (ii) induced no absorber dependence into our detection efficiency (see Sec. IID).

Events which qualified as $\pi\mu e$ decays occurred about once in a thousand pictures during the search for $K^+ \rightarrow \pi^+ \nu \bar{\nu}$, while about one-third of the pictures contained μe decays. The other two-thirds of the pictures were either of particles which stopped in $\pi 3$ or of particles which stopped in the decay counters and showed no evidence of a decay (stopping e^+ , very long-lived μ^+ , and particles which scattered out the sides of the decay counters). In calibration film ($K^+ \rightarrow \pi^+ \pi^0$ and $K^+ \rightarrow \mu^+ \nu$) an event appeared in about every fifth picture.

3. Measurement of Ranges

The range of a K^+ decay particle was determined from the location of the stopping K^+ , the location of the stopping π or μ , and the track direction as shown by the spark-chamber photographs. Scattering in the absorber was taken into account by breaking the track into two straight-line segments whenever it was difficult to fit the spark-chamber tracks with a single straight line. With this procedure it was possible to obtain satisfactory fits for all but about 4% of the events.

We checked the validity of our method by observing the range distributions of the π^+ and μ^+ from the monoenergetic decays $K^+ \rightarrow \pi^+ \pi^0$ and $K^+ \rightarrow \mu^+ \nu$. In Fig. 4(b) these distributions are shown together with the calculated range distributions for these decays. The calculated distributions include the effects of straggling and multiple scattering. The agreement between the observed and calculated distributions indicate that the approximations which we used were entirely satisfactory.

This check establishes that on the average our range measurement yields a correct result. For individual events we know in which of the K -stop counters the particle originated, but we do not know the position of the event within the counter; hence the range which we assign to the event may be in error by as much as 1.2 g/cm^2 . We allowed for this uncertainty in choosing the range criterion by which we distinguished " $K^+ \rightarrow \pi^+ \nu \bar{\nu}$ " events from $K^+ \rightarrow \pi^+ \pi^0$ (see Sec. III).

D. Detection Efficiency

The quantity measured in this experiment is the

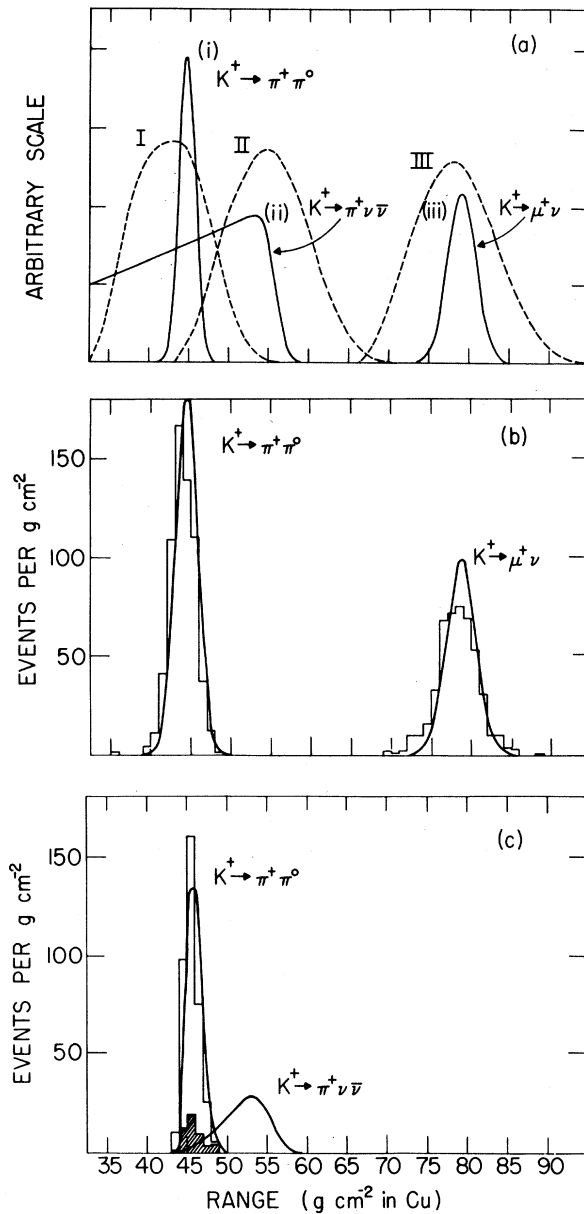


FIG. 4. Range distributions in search for $K^+ \rightarrow \pi^+ \nu \bar{\nu}$: (a) "Ideal" spectra $F(r)$ for K^+ decays into (i) $\pi^+ \pi^0$, (ii) $\pi^+ \nu \bar{\nu}$ (vector), and (iii) $\mu^+ \nu$ with straggling and small-angle multiple scattering taken into account. Dashed curves show detector efficiencies for absorber thicknesses used to detect (I) $K^+ \rightarrow \pi^+ \pi^0$, (II) $K^+ \rightarrow \pi^+ \nu \bar{\nu}$, and (III) $K^+ \rightarrow \mu^+ \nu$ (curve II is weighted sum of curves corresponding to two nearly equal thicknesses). (b) Expected event distributions for $\pi^+ \pi^0$ and $\mu^+ \nu$ and corresponding observed distributions (histograms). The curves are normalized to the observed number of events. (c) Expected $\pi^+ \pi^0$ and $\pi^+ \nu \bar{\nu}$ range distributions for absorber corresponding to curve II, Fig. 4(a), and observed distributions for events satisfying final selection criteria (Sec. III B). [$\gamma C 1$ and/or $\gamma C 2$ required in coincidence for $\pi^+ \pi^0$ (open histogram) and in anticoincidence for " $\pi^+ \nu \bar{\nu}$ " (shaded histogram)].

ratio $\Gamma(K^+ \rightarrow \pi^+ \nu \bar{\nu})/\Gamma(K^+ \rightarrow \pi^+ \pi^0)$, and the known³⁸ branching ratio of $K^+ \rightarrow \pi^+ \pi^0$ is then used to calculate $\Gamma(K^+ \rightarrow \pi^+ \nu \bar{\nu})/\Gamma(K^+ \rightarrow \text{all})$. It is therefore not necessary to calculate the absolute π^+ detection efficiency. We need only consider those effects which influence the relative detection efficiency for π^+ from $K^+ \rightarrow \pi^+ \nu \bar{\nu}$ and from $K^+ \rightarrow \pi^+ \pi^0$. These effects are (i) the dependence of detection efficiency on π^+ range for a given absorber thickness (Sec. IID 1), (ii) the dependence of the π^+ transmission on the absorber thickness (Sec. IID 2), and (iii) the dependence of the scanning efficiency on absorber thickness due to the resultant change in event rate (Sec. IID 3).

1. Efficiency vs π^+ Range

Since the pions from $K^+ \rightarrow \pi^+ \nu \bar{\nu}$ are not monoenergetic, it is necessary to determine the variation of the detector efficiency with the residual range of the pions emerging from the absorber. Prior to the experiment we verified that the outputs of the decay counters did not significantly depend on the location at which energy was deposited in the counters. Hence we computed the variation of efficiency with particle range as a purely geometric quantity.

We have checked our calculation empirically by measuring the π^+ rates from $K^+ \rightarrow \pi^+ \pi^0$ for three different absorber thicknesses. As an additional check we have measured the ratio of the μ^+ rate from $K^+ \rightarrow \mu^+ \nu \gamma$ to that from $K^+ \rightarrow \mu^+ \nu$, where the μ^+ from $K^+ \rightarrow \mu^+ \nu \gamma$ were taken from the same range interval in which we searched for $K^+ \rightarrow \pi^+ \nu \bar{\nu}$. This measurement agrees with the calculated value (see Sec. II E) and provides a direct check on our geometrical calculation.

2. Absorption of π^+

Approximately 39% of the π^+ which originate in the K -stop counters are absorbed before they reach the decay counters. However, it is not necessary to make a direct calculation of this entire correction, since we measure only the ratio $\Gamma(K^+ \rightarrow \pi^+ \nu \bar{\nu})/\Gamma(K^+ \rightarrow \pi^+ \pi^0)$. The transmission, $T_{\pi^+ \pi^0}$, of π^+ for the absorber configuration used to stop pions from $K^+ \rightarrow \pi^+ \pi^0$ is already contained in the measured rate for that reaction. We need only calculate the ratio $T_{\pi^+ \nu \bar{\nu}}/T_{\pi^+ \pi^0}$, which is just the transmission through the extra absorber (11.2 g/cm²) added for detection of $K^+ \rightarrow \pi^+ \nu \bar{\nu}$. This calculation was made using inelastic π^+ nuclear cross sections calculated by Bertini.³⁹ We obtained the value $T_{\pi^+ \nu \bar{\nu}}/T_{\pi^+ \pi^0} = 0.94 \pm 0.01$.

We checked our method of making this calculation by also calculating $T_{\pi^+ \pi^0} = 0.69 \pm 0.02$ and comparing

this figure with the value which could be inferred from our measurement of the ratio $\Gamma(K^+ \rightarrow \pi^+ \pi^0)/\Gamma(K^+ \rightarrow \mu^+ \nu)$ (see Sec. II E).

3. Scanning Efficiency

We expect that the scanning efficiency will be different for $K^+ \rightarrow \pi^+ \pi^0$ and $K^+ \rightarrow \pi^+ \nu \bar{\nu}$, since $\pi \mu e$ events occur on the film at different rates for the two measurements (~ 1 event/5 pictures for $\pi^+ \pi^0$ and ~ 1 event/1000 pictures for $\pi^+ \nu \bar{\nu}$). Conversely, we expect the scanning efficiencies to be comparable for $K^+ \rightarrow \pi^+ \pi^0$ and $K^+ \rightarrow \mu^+ \nu$ ($\sim 3 \mu e$ events/5 pictures).

The possibility of a correlation between range and scanning efficiency for a given absorber thickness was experimentally ruled out by establishing that scanners found $K^+ \rightarrow \pi^+ \pi^0$ events with equal efficiency in each of the four decay counters.

All $K^+ \rightarrow \pi^+ \nu \bar{\nu}$ film was triple scanned, and the Derenzo-Hildebrand technique⁴⁰ was used to estimate the scanning efficiency $S_{\pi^+ \nu \bar{\nu}}$. We obtained a value of 0.98 ± 0.02 for three scans. The normal Geiger-Werner technique⁴¹ was also applied to the first two scans. Three new events were found in the third scan, as compared with 72 in the first two scans. Had we used the Geiger-Werner procedure alone, we would have underestimated the number of events in the film by $\sim 6\%$, which is smaller than our statistical error ($\sim 10\%$). We therefore concluded that a fourth scan was unnecessary.

The efficiencies found for the $K^+ \rightarrow \pi^+ \pi^0$ film (10% triple scanned, 90% double scanned) and for the $K^+ \rightarrow \mu^+ \nu$ film (50% double scanned, 50% single scanned) were $S_{\pi^+ \pi^0} = 0.99 \pm 0.01$ and $S_{\mu^+ \nu} = 0.98 \pm 0.02$.

E. Method of Calculating Branching Ratio

We calculated the branching ratio from the equation

$$\frac{\Gamma(K^+ \rightarrow \pi^+ \nu \bar{\nu})}{\Gamma(K^+ \rightarrow \text{all})} = \frac{(\pi^+ \nu \bar{\nu}/K^+) \epsilon_{\pi^+ \pi^0} T_{\pi^+ \pi^0} S_{\pi^+ \pi^0}}{(\pi^+ \pi^0/K^+) \epsilon_{\pi^+ \nu \bar{\nu}} T_{\pi^+ \nu \bar{\nu}} S_{\pi^+ \nu \bar{\nu}}} \times \frac{\Gamma(K^+ \rightarrow \pi^+ \pi^0)}{\Gamma(K^+ \rightarrow \text{all})}. \quad (3)$$

Here $(\pi^+ \nu \bar{\nu}/K^+)$ is the number of $\pi^+ \nu \bar{\nu}$ events found divided by the corresponding number of K^+ signals, and $(\pi^+ \pi^0/K^+)$ is the corresponding ratio for $\pi^+ \pi^0$ events. The scanning and selection criteria imposed were identical for the samples of $\pi^+ \nu \bar{\nu}$ and $\pi^+ \pi^0$ events. For $\pi^+ \nu \bar{\nu}$ events the triggering mode was $KX^+ \bar{\gamma}$ (see Sec. II B), and the absorber was that corresponding to curve II in Fig. 4(a); for $\pi^+ \pi^0$ the triggering mode was KX^+ , and the absorber was that corresponding to curve I in Fig. 4(a). The

quantities $\epsilon_{\pi^+\pi^0}$ and $\epsilon_{\pi^+\nu\bar{\nu}}$ are the geometrical effective detection efficiencies for $K^+ \rightarrow \pi^+\pi^0$ and $K^+ \rightarrow \pi^+\nu\bar{\nu}$, respectively (see Sec. IID 1). Note that $\epsilon_{\pi^+\nu\bar{\nu}}$ contains the effects of a range selection criterion (see Sec. IIIB) and assumptions about the shape of the pion spectrum (Sec. IIIC). The ratio $T_{\pi^+\pi^0}/T_{\pi^+\nu\bar{\nu}}$ is the correction for π^+ absorption (see Sec. IID 2), and $S_{\pi^+\pi^0}$ and $S_{\pi^+\nu\bar{\nu}}$ are the scanning efficiencies for $K^+ \rightarrow \pi^+\pi^0$ and $K^+ \rightarrow \pi^+\nu\bar{\nu}$, respectively (see Sec. IID 3).

We checked this calculation in two ways. First, we measured the π^+ rate from $K^+ \rightarrow \pi^+\pi^0$ and the μ^+ rate from $K^+ \rightarrow \mu^+\nu$. We then calculated the relative branching ratio $\Gamma(K^+ \rightarrow \pi^+\pi^0)/\Gamma(K^+ \rightarrow \mu^+\nu)$ using the formula

$$\frac{\Gamma(K^+ \rightarrow \pi^+\pi^0)}{\Gamma(K^+ \rightarrow \mu^+\nu)} = \frac{(\pi\pi^0/K^+)}{(\mu^+\nu/K^+)} \frac{\epsilon_{\mu^+\nu}}{\epsilon_{\pi^+\pi^0}} \frac{1}{T_{\pi^+\pi^0}} \frac{S_{\mu^+\nu}}{S_{\pi^+\pi^0}} \frac{1}{C_\pi}.$$

The quantity C_π (0.65 ± 0.06) is the fraction of $\pi^+ \rightarrow \mu^+\nu$ decays for which the stopping π^+ pulse and the $\pi \rightarrow \mu$ decay pulse were sufficiently resolved. This was determined empirically from the pion-lifetime distribution for $K^+ \rightarrow \pi^+\pi^0$ events. The effective-detection efficiencies were $\epsilon_{\pi^+\pi^0} = 0.054$ and $\epsilon_{\mu^+\nu} = 0.046$. The scanning-efficiency correction $S_{\mu^+\nu}/S_{\pi^+\pi^0}$ was 0.98 ± 0.02 . The calculated pion transmission was $T_{\pi^+\pi^0} = 0.69 \pm 0.02$. From the measured event rates, $(\mu^+\nu/K^+) = (1.20 \pm 0.09) \times 10^{-2}$ and $(\pi^+\pi^0/K^+) = (2.10 \pm 0.12) \times 10^{-3}$, we obtained a value of 0.33 ± 0.05 for the relative branching ratio. A second measurement, made with slightly different apparatus geometry and with minor changes in the electronics, gave an identical result. The weighted average of these two measurements is 0.33 ± 0.03 , which is in good agreement with the accepted value,³⁸ 0.33.

As a second check we measured the event rate of μ^+ from $K^+ \rightarrow \mu^+\nu\gamma$ relative to the rate for $K^+ \rightarrow \mu^+\nu$. The measured ratio, $(1.16 \pm 0.17) \times 10^{-3}$, was found to be in good agreement with the expected ratio, $(1.08 \pm 0.05) \times 10^{-3}$. The expected ratio was obtained by folding the calculated efficiency into the spectrum $[\Gamma(K^+ \rightarrow \mu^+\nu)]^{-1} d\Gamma(K^+ \rightarrow \mu^+\nu\gamma)/dT$ from a calculation by Cabibbo,⁴² taking straggling and multiple scattering into account. It was necessary to reduce the ratio obtained in this way by a small amount (12%) to account for events for which the γ ray was vetoed by the γC counters. This was done using the known⁴² angular distribution of the γ rays. The error quoted for the predicted ratio is an estimate of the uncertainty in this correction.

III. RESULTS

The results are presented in Tables III and IV. The limits shown in these tables differ somewhat from those in the preliminary publications^{1,2} be-

cause of an improved calculation of the detection efficiencies. The limit for $K^+ \rightarrow \pi^+\nu\bar{\nu}$ (vector), for example, has been raised from 1.2×10^{-6} to 1.4×10^{-6} . The previous calculation did not properly allow for distortions in the assumed spectra due to straggling.

Figure 5 shows the range distribution of all $\pi\mu e$ events found by the scanners during the search for $K^+ \rightarrow \pi^+\nu\bar{\nu}$. Those events with a range of at least 50 g/cm² in Cu were termed " $K^+ \rightarrow \pi^+\nu\bar{\nu}$ " events. Since the range distribution extends well above the kinematic upper limit for $K^+ \rightarrow \pi^+\nu\bar{\nu}$, it is clear that at least some of the events are not examples of this decay. We must therefore inquire, what are the possible sources of background, and what experimental cuts can we make to reduce this background.

A. Sources of Background

Background events in the sample of " $K^+ \rightarrow \pi^+\nu\bar{\nu}$ " may be included either through misidentifying muons as pions or by observing pions from some source other than reaction (1).

1. Misidentified Events

About $\frac{1}{3}$ of all the pictures taken during the search for $K^+ \rightarrow \pi^+\nu\bar{\nu}$ contained stopping μ^+ (from $K^+ \rightarrow \pi^0\mu^+\nu$ and $K^+ \rightarrow \mu^+\nu\gamma$). The most likely source of accidental background consisted of mistaking one of these μe decays for a $\pi\mu e$ decay because of an accidental pulse in a decay counter (e.g., made by a Compton electron from an accidental γ). We measured the frequency with which these misidentifications occurred by scanning 60 000 pictures of stop-

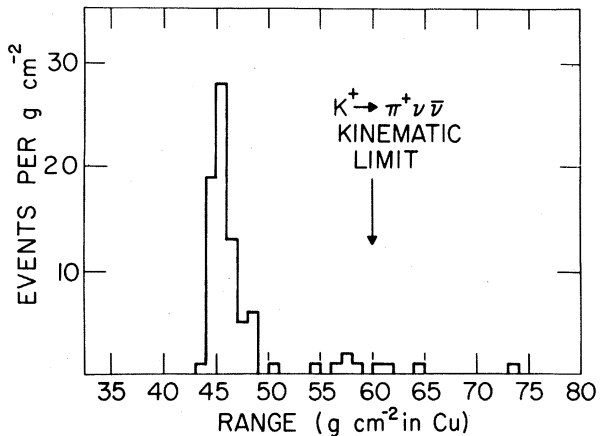


FIG. 5. Range distribution of events found by scanners during search for $K^+ \rightarrow \pi^+\nu\bar{\nu}$ with no cuts on $\pi\mu$ pulse height or on π or μ lifetimes. The arrow indicates the kinematic limit for $K^+ \rightarrow \pi^+\nu\bar{\nu}$ (including straggling). We would not expect events from $K^+ \rightarrow \pi^+\pi^0$ above 50 g/cm² [see Fig. 4(c)].

ping μ^+ from $K^+ \rightarrow \mu^+ \nu$ for " $\pi\mu e$ " events. Here the measured range of the stopping particle ($R > 70$ g/cm²) was well above the maximum range possible for a π^+ produced by a decaying K^+ , while the large branching ratio of the $\mu^+ \nu$ decay mode made the probability of a scattered beam π^+ negligible. These pictures were taken at the maximum beam intensity and with the same apparatus geometry used in searching for reaction (1). The sample of spurious $\pi\mu e$ was then used to predict the expected background from misidentified μ^+ as a function of the experimental cuts (see Sec. III B). The known spectrum of the stopping muons was taken into account. We verified that these events resulted from an accidental process associated with the beam by repeating the measurement for 23 500 pictures taken with the beam intensity reduced by a factor of ten. No $\pi\mu e$ events were found in these pictures.

2. Other Sources of π^+

There are two known sources of π^+ other than K^+ decays. One is π^+ which scatter out of the beam (see Sec. III A 2a). The other is $K_L^0 \rightarrow \pi^+ e^- \nu$, where the K^0 is made from a K^+ by charge exchange in one of the K -stop counters. We estimate that this source of background is negligible (see Sec. III A 2b). Since our experiment sets only an upper limit on the branching ratio for $K^+ \rightarrow \pi^+ \nu \bar{\nu}$, our result does not depend on this estimate.

(a) *Scattered beam π^+ .* Our triggering criteria were such that the following conditions would be required in order for a scattered π^+ to be mistaken for a K^+ decay product: A K^+ must stop in one of the K -stop counters and decay in such a way that none of its decay products is detected by our counters. A π^+ must then enter the apparatus between 6 and 54 nsec later, undergo an inelastic nuclear scatter in one of the K -stop counters, and stop in one of the decay counters.

In the course of the experiment several minor changes were made in the apparatus to improve our identification of scattered π^+ . During the portion of the run for which this identification was most reliable, one scattered π^+ was observed in 6.4×10^8 K^+ signals (about $\frac{1}{2}$ of the total for the experiment). This event was the basis for our estimate of the background of scattered π^+ for the whole run, which was 1.8 events for the set of event-selection criteria to be adopted in the next section.

(b) *Pions from $K_L^0 \rightarrow \pi^+ e^- \nu$.* Pions produced by $K_L^0 \rightarrow \pi^+ e^- \nu$ have a range spectrum like that assumed for $K^+ \rightarrow \pi^+ \nu \bar{\nu}$. No such events were observed. Because of our timing requirement on K -decay products, only very low-energy K^0 would remain in the region of the K -stop counters until

our π detector became sensitive (6 nsec after the K^+ stop). In addition, the $K4$ and $K5$ counters would veto a large fraction of the e^- produced in $K_L^0 \rightarrow \pi^+ e^- \nu$.

It is difficult to estimate the effect of the timing requirement. To satisfy the requirement the K^0 would have to be produced with energy less than 600 keV, and the cross section for a K^+ of energy

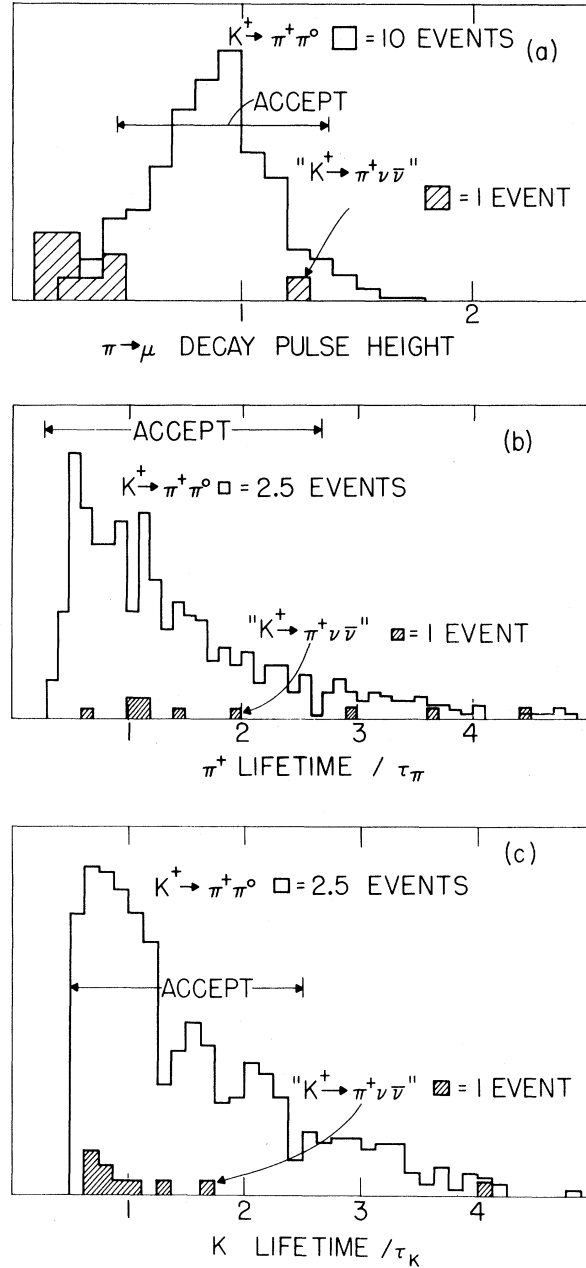


FIG. 6. Characteristics of " $K^+ \rightarrow \pi^+ \nu \bar{\nu}$ " events (shaded histograms) compared with those of $K^+ \rightarrow \pi^+ \pi^0$ events (open histograms). (a) Muon pulse-height distributions. (b) Pion lifetime distributions. (c) Kaon lifetime distributions.

E striking a carbon nucleus to produce such a K^0 is unknown. We have estimated this cross section by assuming that the carbon nucleus was composed of six deuterons, each of which acted independently. The measured K^+d charge-exchange cross section⁴³ was then linearly extrapolated to the energy for which the K^0 would be produced with 600 keV, and six times this cross section was used in our estimate. On the basis of these assumptions and taking into account the suppression of e^- , we have concluded that the probability of such a background was negligible.

B. Event Selection Criteria and Final Sample

We may reduce the background by imposing appropriate selection criteria on events which satisfy the scanning criteria. We select events on the basis of μ pulse height, π lifetime, and K lifetime. The first two of these criteria suppress background events from misidentified μe 's, since the accidental " $\pi\mu$ decay" pulses will not have height or time distributions like those for $K^+ \rightarrow \pi^+ \mu^+ \rightarrow e^+$. The third criterion reduces the background from scattered beam pions.

In Fig. 6 the measured μ -pulse-height, π -lifetime, and K -lifetime distributions are shown for $K^+ \rightarrow \pi^+ \pi^0$ events (open histograms) and for the initial sample of " $K^+ \rightarrow \pi^+ \nu\bar{\nu}$ " events (shaded histograms). The final selection criteria chosen are also indicated in this figure. The criteria were chosen to maximize our sensitivity to $K^+ \rightarrow \pi^+ \mu^+ \rightarrow e^+$ decays, as empirically determined from the $K^+ \rightarrow \pi^+ \pi^0$ events, over the background estimated from independent measurements, as described in Secs. III A 1 and III A 2 a above. We

stress that this choice was made independently of the " $K^+ \rightarrow \pi^+ \nu\bar{\nu}$ " sample. It is evident that the elimination of very small " μ " pulses is the most important selection criterion. For $K^+ \rightarrow \pi^+ \pi^0$ events the measured π^+ lifetime is 26.3 ± 1.3 nsec, in good agreement with the accepted value, $26.3 \pm .06$ nsec.

It is important to establish that our result does not depend on the way in which we chose our event selection criteria. Table II shows the number of " $K^+ \rightarrow \pi^+ \nu\bar{\nu}$ " events found and the expected number of background events from misidentified μe 's and scattered-beam pions for a wide variety of selection criteria. We see from this table that the signal is consistent with the expected background in all cases, and that the sole effect of our selection criteria is to maximize our experimental sensitivity. The excess of estimated background over events is presumably due to statistical fluctuations. (The background estimate is based on a sample of 4 to 7 events, depending on the selection criteria.) Note that the various background estimates are not independent.

In Fig. 4(c) the range distribution of those $\pi\mu e$ events in the initial sample (Fig. 5) which satisfied our event selection criteria (shaded histogram) is compared with the observed $K^+ \rightarrow \pi^+ \pi^0$ range distribution (open histogram), with the expected range distribution for $K^+ \rightarrow \pi^+ \pi^0$, and with the expected range distribution for $K^+ \rightarrow \pi^+ \nu\bar{\nu}$. We conclude from this that we have observed no examples of reaction (1).

C. Interpretation of Result

1. First-Order Theories

In order to express our result as an upper limit

TABLE II. Accepted " $K^+ \rightarrow \pi^+ \nu\bar{\nu}$ " candidates and expected background for various selection criteria.

Selection criteria ^a				" $K^+ \rightarrow \pi^+ \nu\bar{\nu}$ " events	Expected background
$\pi \rightarrow \mu$ decay pulse height ^b		π lifetime ^c	K lifetime ^c		
Lower limit	Upper limit				
none ^a	none	none	none	7	7.4
0.3	none	none	none	5	7.4
0.3	1.7	none	none	5	7.4
0.3	1.7	none	$< 2\tau_K$	2	5.5
0.3	1.7	$< 2\tau_\pi$	$< 2\tau_K$	0	3.7
0.5	1.5	none	none	4	5.6
0.5	1.5	$< 2\tau_\pi$	none	3	4.3
0.5	1.5	$< 3\tau_\pi$	$< 2\tau_K$	1	2.4
0.5	1.5	$< 2\tau_\pi$	$< 3\tau_K$	1	3.4
0.5 ^d	1.5 ^d	$< 2\tau_\pi$	$< 2\tau_K$	0	2.4

^aImposed in addition to the scanning and analysis criteria, which include a lower limit on $\pi \rightarrow \mu$ decay pulse height (see Secs. II C 2 and II D 3).

^bMeasured in units of mean $\pi \rightarrow \mu$ decay pulse height.

^cMeasured from the experimental threshold.

^dThese are the selection criteria adopted (see Sec. III B).

on the branching ratio $\Gamma(K^+ \rightarrow \pi^+ \nu \bar{\nu})/\Gamma(K^+ \rightarrow \text{all})$, using Eq. (3), we must make assumptions about the shape of the π^+ spectrum in order to calculate the effective detection efficiency, $\epsilon_{\pi^+ \nu \bar{\nu}}$. For a first-order theory with constant form factors there are three possible spectral shapes.⁴⁴ These are listed in Table III with the corresponding detection efficiencies and branching ratio limits. We have taken as the 90% confidence limit the branching ratio which we would compute had we found 2.3 events. The values appearing in the table were calculated from Eq. (3) using the following numerical values for the various terms: $(\pi^+ \nu \bar{\nu}/K^+) = 1.47 \times 10^{-9}$ (assuming 2.3 events); $(\pi^+ \pi^0/K^+) = (1.26 \pm 0.06) \times 10^{-3}$ (identical selection criteria were applied to both " $K^+ \rightarrow \pi^+ \nu \bar{\nu}$ " and $K^+ \rightarrow \pi^+ \pi^0$ events); $T_{\pi^+ \pi^0}/T_{\pi^+ \nu \bar{\nu}} = 1.06 \pm 0.01$; $\epsilon_{\pi^+ \pi^0} = 0.054$; $S_{\pi^+ \pi^0}/S_{\pi^+ \nu \bar{\nu}} = 1.02 \pm 0.02$; $\Gamma(K^+ \rightarrow \pi^+ \pi^0)/(K^+ \rightarrow \text{all}) = 0.21$.

2. Other Theories

For theories which predict the occurrence of reaction (1) as a higher-order weak process, or for first-order theories with rapidly-varying form factors, the π^+ energy spectrum may differ considerably from those in Table III. We therefore present the following prescription for obtaining the upper limit to be inferred from our result for any given spectrum. In Fig. 7 we display the differential detection efficiency $H(T)$ as a function of T_π , where $H(T)$ is defined by

$$\frac{\epsilon_{\pi^+ \nu \bar{\nu}}}{\epsilon_{\pi^+ \pi^0}} = \int_{111 \text{ MeV}}^{153 \text{ MeV}} H(T) F(T) dT.$$

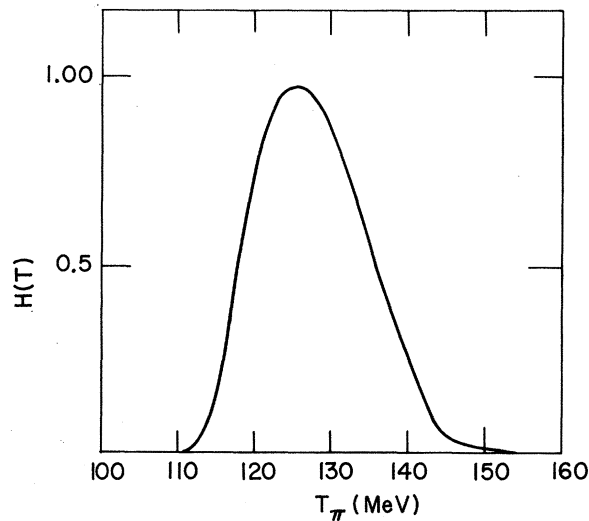


FIG. 7. $K^+ \rightarrow \pi^+ \nu \bar{\nu}$ differential detection efficiency: The function $H(T)$ for $K^+ \rightarrow \pi^+ \nu \bar{\nu}$ as described in Sec. III C 2.

TABLE III. Effective detection efficiency $\epsilon_{\pi^+ \nu \bar{\nu}}$ ($R_\pi > 50 \text{ g cm}^{-2}$) and resultant branching ratio (90% C.L.) for several assumed π^+ spectra. p_π and T_π are the momentum and kinetic energy, respectively, of the π^+ . $T_M = 127 \text{ MeV}$ is the kinematic upper limit for $K^+ \rightarrow \pi^+ \nu \bar{\nu}$. The spectra were normalized to have unit area between 0 and T_M .

$\frac{dN}{dT_\pi}$ assumed	Type of first-order interaction	$\epsilon_{\pi^+ \nu \bar{\nu}}$ ^a	$\frac{\Gamma(K^+ \rightarrow \pi^+ \nu \bar{\nu})}{\Gamma(K^+ \rightarrow \text{all})}$ ^a
p_π^3	vector	0.0103	$< 1.4 \times 10^{-6}$
$p_\pi^3(T_M - T_\pi)$	tensor	0.0014	$< 1.0 \times 10^{-5}$
$p_\pi(T_M - T_\pi)$	scalar	0.00059	$< 2.6 \times 10^{-5}$

^aThese numbers differ from the preliminary results (Ref. 1). The earlier values for the detection efficiency did not properly allow for distortions in the assumed spectra due to straggling.

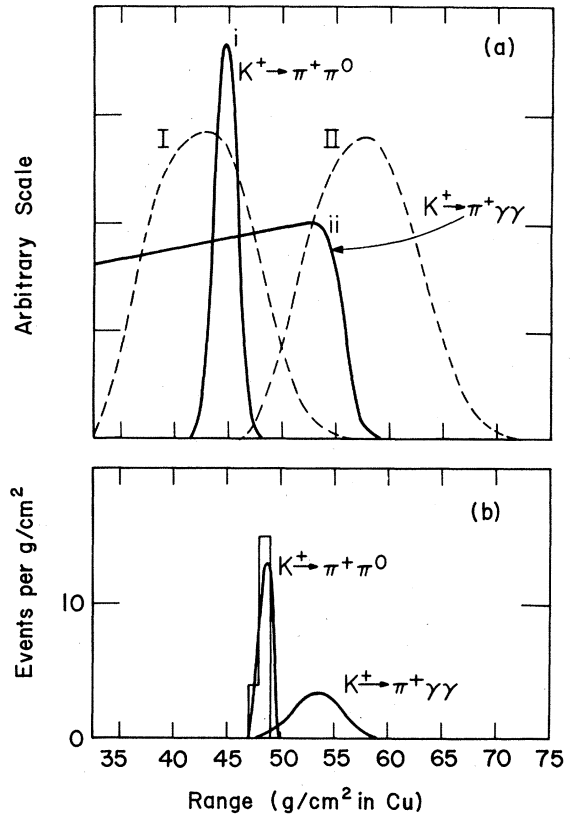


FIG. 8. Range distributions in search for $K^+ \rightarrow \pi^+ n \gamma$. (a) Calculated distributions for K^+ decays into (i) $\pi^+ \pi^0$, and (ii) $\pi^+ \gamma \gamma$ (phase space), with straggling and small-angle multiple scattering taken into account. Dashed curves I and II show detector efficiencies for different absorber thicknesses. (b) Expected $\pi^+ \pi^0$ and " $\pi^+ \gamma \gamma$ " distributions (curves) for absorber corresponding to curve II, Fig. 4(a), together with observed distribution (histogram) of events found during search for $K^+ \rightarrow \pi^+ n \gamma$ (no " $\pi^+ n \gamma$ " events above $\pi^+ \pi^0$ curve).

[The effects of straggling, multiple scattering, and range selection ($R \geq 50$ g/cm²) are contained in $H(T)$.] The function $F(T)$ is the pion energy spectrum from $K^+ \rightarrow \pi^+ \nu \bar{\nu}$, normalized such that

$$\int_0^{127 \text{ MeV}} F(T) dT = 1.$$

From $H(T)$ the corresponding relative detection efficiency $\epsilon_{\pi^+ \nu \bar{\nu}}/\epsilon_{\pi^+ \pi^0}$ can be obtained for any given π^+ spectrum, and the corresponding upper limit to be inferred from our experiment can then be calculated from Eq. (3) and the numerical values given in Sec. III C 1.

D. $K^+ \rightarrow \pi^+ n\gamma$

We searched for $K^+ \rightarrow \pi^+ n\gamma$ in the same way as for $K^+ \rightarrow \pi^+ \nu \bar{\nu}$, except that the triggering mode was KX^+ instead of $KX^+ \bar{\gamma}$ (see Sec. II B). Just as with $K^+ \rightarrow \pi^+ \nu \bar{\nu}$, we would classify any π^+ found with range above 50 g/cm² as a " $K^+ \rightarrow \pi^+ n\gamma$ " event. Fig. 8(b) shows the sample of all events which satisfied the scan cuts; since this sample contains no " $K^+ \rightarrow \pi^+ n\gamma$ " events, no further selection criteria were necessary. The estimated background was 0.7 events. The number of stopping K^+ in this experiment was 9×10^7 , or about $\frac{1}{20}$ the number in the search for $K^+ \rightarrow \pi^+ \nu \bar{\nu}$. The measured event rates were $(\pi^+ n\gamma/K^+) = 2.49 \times 10^{-8}$ (assuming 2.3 events) and $(\pi^+ \pi^0/K^+) = 1.68 \times 10^{-3}$. The scanning efficiency was $S_{\pi^+ n\gamma} = 0.99 \pm 0.01$ and the correction for π^+ absorption was $T_{\pi^+ \pi^0}/T_{\pi^+ n\gamma} = 1.17 \pm 0.01$. The branching ratio was computed using Eq. (3) and the numerical values for $\Gamma(K^+ \rightarrow \pi^+ \pi^0)$ and $\epsilon_{\pi^+ \pi^0}$ given in Sec. III C 1.

In all cases except $n=1$, for which our result is independent of model, we have assumed a constant matrix element (i.e., a "phase-space" model), which gives the spectrum

TABLE IV. Effective detection efficiency and resultant upper limit (90% confidence level) on the branching ratio $K^+ \rightarrow \pi^+ n\gamma$ for several values of n . For $n > 1$ we assume a phase space model for the decay, i.e., $dN/dT_\pi = \lambda p_\pi \times (T_M - T_\pi)^{n-2}$, where p_π and T_π are the momentum and kinetic energy of the π^+ , $T_M = 127$ MeV is the kinematic upper limit for $K^+ \rightarrow \pi^+ n\gamma$, and λ is a constant.

n	Reaction	$\epsilon_{\pi^+ n\gamma}$	Branching ratio
1	$K^+ \rightarrow \pi^+ \gamma$	0.054	$< 4 \times 10^{-6}$
2	$K^+ \rightarrow \pi^+ \gamma \gamma$	0.0045	$< 5 \times 10^{-5}{}^a$
3	$K^+ \rightarrow \pi^+ \gamma \gamma \gamma$	0.00059	$< 3 \times 10^{-4}$

^aThe branching ratio for $n=2$ differs somewhat from that given in the preliminary publication ($< 4 \times 10^{-5}$; see Ref. 2). The earlier value was based on a calculation of the detection efficiency which did not properly allow for distortion of the assumed spectrum due to straggling.

$$d\Gamma(K^+ \rightarrow \pi^+ n\gamma)/dT_\pi = \lambda p_\pi (T_M - T_\pi)^{n-2},$$

where λ is constant. For $n=2$, $\epsilon_{\pi^+ \gamma \gamma} = 4.5 \times 10^{-3}$, and we compute

$$\frac{\Gamma(K^+ \rightarrow \pi^+ \gamma \gamma)}{\Gamma(K^+ \rightarrow \text{all})} < (4.5 \pm 0.03) \times 10^{-5}$$

at the 90% confidence level. The branching ratios corresponding to other values of n are displayed in Table IV.

The differential detection efficiency $I(T)$ for $K^+ \rightarrow \pi^+ n\gamma$ (see Fig. 9) is defined such that

$$\frac{\epsilon_{\pi^+ n\gamma}}{\epsilon_{\pi^+ \pi^0}} = \int_{111 \text{ MeV}}^{153 \text{ MeV}} I(T) F(T) dT$$

for any assumed π^+ spectrum $F(T)$, which is normalized to have unit integral between 0 and the $K^+ \rightarrow \pi^+ n\gamma$ kinematic limit. From this and the numerical values given above, it is possible to infer an upper limit on the $K^+ \rightarrow \pi^+ n\gamma$ branching ratio from our result for any given theoretical model.

ACKNOWLEDGMENTS

We are grateful to Professor E. Segrè for his encouragement and support and to Dr. C. Wiegand and D. Brandshaft for valuable assistance, especially in the early stages of this experiment. We also wish to thank W. Davis, J. Gallup, N. Green, E. Hahn, D. Hildebrand, P. Newman, and J. Wild for their help with scanning, analysis, and operation. We are grateful to the operating crew of the Bevatron for their cooperation during the experi-

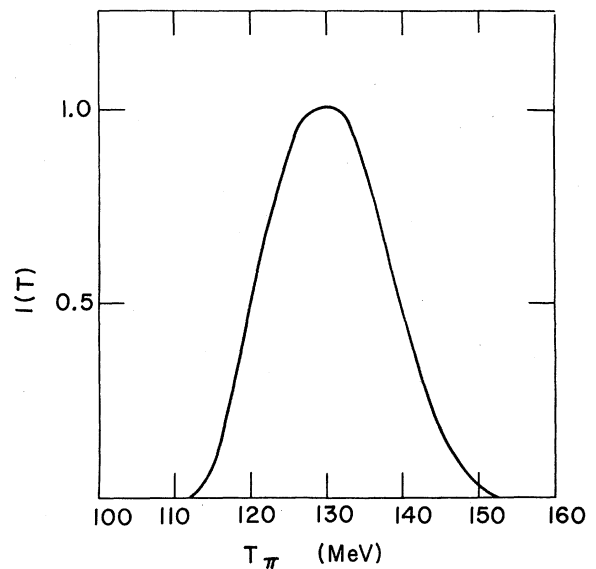


FIG. 9. $K^+ \rightarrow \pi^+ n\gamma$ differential detection efficiency: the function $I(T)$ for $K^+ \rightarrow \pi^+ n\gamma$ as described in Sec. III D.

mental run. One of us (R.H.H.) wishes to acknowledge with thanks his support by the John Simon

Guggenheim Foundation during the course of this experiment.

*Research supported by the U. S. Atomic Energy Commission and by the National Science Foundation under Grant No. GP 14521.

†This work is the subject of a thesis submitted by J. H. Klems in partial fulfillment of the requirements of the Doctor of Philosophy degree at the University of Chicago. Present address: Laboratory of Nuclear Studies, Cornell University, Ithaca, N. Y. 14850.

¹J. H. Klems, R. H. Hildebrand, and R. Stiening, *Phys. Rev. Letters* **24**, 1086 (1970).

²J. H. Klems, R. H. Hildebrand, and R. Stiening, *Phys. Rev. Letters* **25**, 473 (1970).

³U. Camerini, D. Ljung, M. Sheaff, and D. Cline, *Phys. Rev. Letters* **23**, 326 (1969). The number quoted is the 90% confidence level.

⁴Yu. V. Galaktionov and E. P. Shabalin, *Zh. Eksperim. i Teor. Fiz. Pis'ma Redaktsiyu* **8**, 600 (1968) [*Soviet Phys. JETP Letters* **8**, 369 (1968)].

⁵U. Camerini, D. Cline, W. F. Fry, and W. M. Powell, *Phys. Rev. Letters* **13**, 318 (1964).

⁶V. Bisi, R. Cester, A. Marzari Chiesa, and M. Vigone, *Phys. Letters* **25B**, 572 (1967).

⁷D. Cline, H. Haggerty, W. Singleton, W. Fry, and N. Schgal, in *Proceedings of the International Conference on Elementary Particles, Heidelberg, Germany, 1967*, edited by H. Filthuth (North-Holland, Amsterdam, 1968).

⁸U. Camerini, D. Cline, G. Gidal, G. Kalmus, and A. Kernan, *Nuovo Cimento* **37**, 1795 (1965).

⁹D. Cline, Ph.D. dissertation, University of Wisconsin, 1965 (unpublished).

¹⁰D. W. Carpenter, A. Abashian, R. J. Abrams, G. P. Fisher, B. M. K. Nefkens, and J. H. Smith, *Phys. Rev.* **142**, 871 (1966).

¹¹V. L. Fitch, R. F. Rota, J. Russ, and W. Vernon, *Phys. Rev.* **164**, 1711 (1967).

¹²M. Bott-Bodenhausen, X. deBouard, D. G. Cassel, D. Dekkers, R. Felst, R. Mermod, I. Savin, P. Scharff, M. Vivargent, T. R. Willetts, and K. Winter, *Phys. Letters* **24B**, 194 (1967).

¹³A. R. Clark, T. Elioff, R. C. Field, H. J. Frisch, R. P. Johnson, L. T. Kerth, and W. A. Wenzel (private communication).

¹⁴C. Aiff-Steinberger, W. Hever, K. Kleinknecht, C. Rubbia, A. Scribano, J. Steinberger, M. J. Tannenbaum, and K. Tittel, *Phys. Letters* **21**, 595 (1966).

¹⁵H. Foeth, M. Holder, E. Radermacher, A. Stande, P. Darriulat, J. Deutsch, K. Kleinknecht, C. Rubbia, K. Tittel, M. I. Ferrero, and C. Grosso, *Phys. Letters* **30B**, 282 (1969).

¹⁶P. Darriulat, M. I. Ferrero, C. Grosso, M. Holder, J. Pilcher, E. Radermacher, C. Rubbia, M. Sitrè, A. Stande, and K. Tittel, *Phys. Letters* **33B**, 249 (1970).

¹⁷B. D. Hyams, W. Koch, D. C. Potter, L. Von Linden, E. Lorenz, G. Lütjens, U. Stierlin, and P. Weilhammer, *Phys. Letters* **29B**, 521 (1969).

¹⁸R. D. Stutzke, A. Abashian, L. H. Jones, P. M. Mantsch, J. R. Orr, and J. H. Smith, *Phys. Rev.* **177**,

2009 (1969).

¹⁹M. M. Block, H. Burmeister, D. C. Cundy, B. Eiben, C. Franzinetti, J. Keren, R. Nollerud, G. Myatt, M. Nikolic, A. Orkin-Lecourtois, M. Paty, D. Perkins, C. A. Ramm, K. Schultz, H. Sletten, K. Soop, R. Stump, W. Venus, and H. Yoshiki, in *Proceedings of the Twelfth International Conference on High-Energy Physics, Dubna, 1964* (Atomizdat, Moscow, USSR, 1966), Vol. 2, p. 7.

²⁰J. H. Munsee and F. Reines, *Phys. Rev.* **177**, 2002 (1969).

²¹R. J. Oakes, *Phys. Rev. Letters* **20**, 1539 (1968).

²²R. J. Oakes, *Phys. Rev.* **183**, 1520 (1969).

²³S. B. Treiman, *Nuovo Cimento* **15**, 916 (1959).

²⁴See, for example, R. Dashen, S. C. Frautschi, and D. H. Sharp, *Phys. Rev. Letters* **13**, 777 (1964); R. Dashen, S. C. Frautschi, M. Gell-Mann, and Y. Hara, Caltech report, 1964 (unpublished).

²⁵For example, see N. Christ, *Phys. Rev.* **176**, 2086 (1968), G. Segrè, *ibid.* **181**, 1996 (1969); M. Gell-Mann, M. L. Goldberger, N. M. Kroll, and F. E. Low, *ibid.* **179**, 1518 (1969); R. S. Willey, *Phys. Rev. D* **1**, 2182 (1970); S. K. Singh and L. Wolfenstein, *Nucl. Phys.* **B24**, 77 (1970); and R. E. Marshak, Y. W. Yang, and J. S. Rao, *Phys. Rev. D* **3**, 1640 (1971).

²⁶For this reason we do not know whether or not the estimate $\Gamma(K^+ \rightarrow \pi^+ + \nu + \bar{\nu}) / \Gamma(K^+ \rightarrow \text{all}) \approx 5 \times 10^{-6}$ made by G. Segrè (see Ref. 25) is in agreement with our result.

²⁷A. Pais and S. B. Treiman, *Phys. Rev.* **176**, 1974 (1968).

²⁸M. Chen, D. Cutts, P. Kijewski, R. Stiening, C. Wiegand, and M. Deutsch, *Phys. Rev. Letters* **20**, 73 (1968).

²⁹N. Cabibbo and R. Gatto, *Phys. Rev. Letters* **5**, 382 (1960).

³⁰Y. Hara and Y. Nambu, *Phys. Rev. Letters* **16**, 875 (1966).

³¹S. Okubo, R. E. Marshak, and V. S. Mathur, *Phys. Rev. Letters* **19**, 407 (1967).

³²Y. Fujii, *Phys. Rev. Letters* **17**, 613 (1966).

³³G. Oppo and S. Oneda, *Phys. Rev.* **160**, 1397 (1967).

³⁴Y. Fujii (private communication).

³⁵G. Faldt, B. Peterson, and H. Pilkuhn, *Nucl. Phys.* **B3**, 234 (1967).

³⁶F. Selleri, *Nuovo Cimento* **60A**, 291 (1969); **57A**, 678 (1968).

³⁷D. Friedell, M. Deutsch, D. Cutts, R. Stiening, and C. Wiegand, MIT Report No. MIT-2098-389, 1967 (unpublished).

³⁸From a compilation by Particle Data Group, *Rev. Mod. Phys.* **42**, 87 (1970).

³⁹H. W. Bertini, *Phys. Rev.* **131**, 1801 (1963); **138**, AB2 (1965); and personal communication.

⁴⁰S. E. Derenzo and R. H. Hildebrand, *Nucl. Instr. Methods* **69**, 287 (1969).

⁴¹H. Geiger and A. Werner, *Z. Physik* **21**, 187 (1924).

⁴²N. Cabibbo, *Nuovo Cimento* **11**, 837 (1959). A measurement of this reaction which agrees with the calcula-

tion (experimental accuracy 30%) has been made by M. Chen, LRL Report No. UCRL-18653, 1969 (unpublished).

⁴³W. Slater, D. H. Stork, H. K. Ticho, W. Lee, W. Chinowsky, G. Goldhaber, S. Goldhaber, and T. O'Halloran,

Phys. Rev. Letters 7, 517 (1961).

⁴⁴This follows by a straightforward calculation from the matrix element given by J. D. Jackson, *Elementary Particle Physics and Field Theory* [1962 Brandeis Summer Institute] (Benjamin, New York, 1963), p. 290.

PHYSICAL REVIEW D

VOLUME 4, NUMBER 1

1 JULY 1971

Muons Produced By Atmospheric Neutrinos: Experiment*

F. Reines, W. R. Kropp, H. W. Sobel, H. S. Gurr, and J. Lathrop
University of California, Irvine, California 92664

and

M. F. Crouch

Case Western Reserve University, Cleveland, Ohio 44106

and

J. P. F. Sellschop and B. S. Meyer†

University of the Witwatersrand, Johannesburg, Republic of South Africa
(Received 8 February 1971)

The interaction of high-energy muon neutrinos produced in the atmosphere by primary cosmic rays has been observed deep underground (8.74×10^5 g cm⁻² std. rock) in the rock surrounding a large-area (160 m²) liquid-scintillation-detector hodoscope. A series of arguments is given to separate the residual atmospheric muons which reached the detector from those produced by neutrino interactions in the surrounding rock. These arguments are based on the widely differing angular distributions and mean energies of the two sources. The observation of four events arising from the decay of muons stopping in the detector suggests that the energy of neutrino-induced muons is $\sim \frac{1}{2}$ GeV. Operation of the system over a three-year period yielded a total of 39 which we identify as neutrino-produced muons. Of these, 35 were in the aperture chosen for the observation of neutrino-induced muons, yielding a total rate of $(6.5 \pm 1.1) \times 10^{-7}$ sec⁻¹. In a companion paper, this result is compared with rates predicted using various theoretical models of the neutrino-nucleon interaction. This comparison selects the most appropriate model and leads to an underground neutrino-induced muon flux. In the present paper the simplifying approximation of an isotropic neutrino distribution leads directly to a flux of $(3.7 \pm 0.6) \times 10^{-13}$ cm⁻² sec⁻¹ sr⁻¹.

I. INTRODUCTION

High-energy neutrinos resulting from the interaction of primary cosmic rays with the earth's atmosphere have long been considered a possible tool for the investigation of the weak interaction.¹⁻³ Interest in such experiments was heightened with the discovery of the accelerator-produced, muon-associated neutrino in 1962.⁴ In undertaking the present experiment, it was anticipated that the higher-energy neutrinos available in the secondary cosmic rays might cast light on the question of the existence of a mediating vector boson for the weak interaction as well as reveal something of the character of the interaction cross section for neutrinos with energies in excess of those available at accelerators. In addition to these definable goals was the hope that a more sensitive search for cosmic-

ray neutrinos might yield information as to hitherto unsuspected sources or interactions.

Assuming a cross section in the vicinity of 10^{-38} cm²/nucleon, and calculations of the atmospheric neutrino spectrum and flux based on measurements of atmospheric muons produced in the decay processes associated with these neutrinos, it was estimated by various authors¹⁻³ that a detector of effective mass measuring a few thousand tons would be required to yield a signal of several events per year. Since the neutrino interaction was signaled by a muon, it was immediately evident that, unless special steps were taken, such a large detector would be flooded with a background arising from atmospheric muons which was some 10^{10} times as intense as the expected signal. Two variants to reduce the background below that expected at sea level were the use of a moderate depth in conjunc-

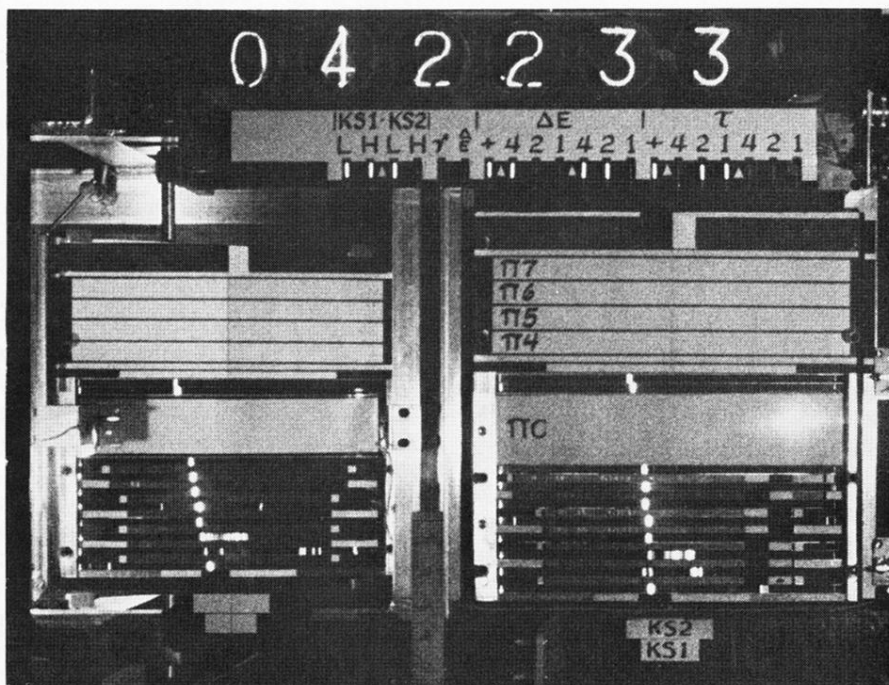


FIG. 2. A $\pi^+ \rightarrow \mu^+ \rightarrow e^+$ event from $K^+ \rightarrow \pi^+ \pi^0$ decay: Two views of the pion track traversing the spark gaps. The right-hand view looks directly at the downstream side of the apparatus; the left-hand view shows the bottom by means of a mirror. Note that the track appears to intersect the K -stop counters in both views. The row of labeled lights just below the event number contains coded information from the triggering system as explained in Sec. II B.